Session 1-3
Chairman : E. Vossenberg, CERN

Switching Technology

REVIEW OF SESSION 1.3 - SWITCHING TECHNOLOGY

Eugene Vossenberg (Chairman)
CERN

1. The Diversified Technologies paper (Michael Kempkes)

The paper describes an IGBT series array used as a solid-state Opening switch for Crowbar application replacement. This is a fast opening, and easily controllable array configuration, and is a good hardware demonstration of the IGBTs opening features.

2. The Marconi Technologies paper (Ron Sheldrake)

This paper gave no surprises except that it did show that thyratron development is still possible for creating low-cost, high-voltage, reliable switching devices. No mention was made of thyratron development for long pulse (100 μs) and high average current applications such as those for the CLIC drive beam klystron-modulators.

3 & 4. The APP Inc (C. Glidden) and ABB Semiconductors (Adriaan Welleman) papers

Thyratron and Ignitron replacement.

These companies proposed alternative solutions to using the thyratron based on interdigitated semiconductor technologies. They showed that rate of current rise of around 30kA/μs and peak currents of up to 100kA at 400 Hz repetition frequency, for pulse widths of several μs is possible. Wafer sizes that are used in this application range from 65 to 90 mm diameter, although for the same di/dt but at peak currents of about 6 kA and 3 μs pulse widths, wafer sizes of around 15 mm diameter are used as well. Operational voltages used are in general about 75% of the installed voltage of the device. Switches of this type are of modular design. Lifetime expectations are good although reliability data and field experience are still short. Availability of these devices and their costs will come down as volume production improves. Questions that are uppermost in the designers mind are: Does one make the switch circuit development in-house, or provide a good specification based on realistic simulations and fault analysis situations for development of an appropriate device for the circuit at the semiconductor manufacturers? What are the long-term maintenance implications?

A SOLID STATE OPENING SWITCH FOR CROWBAR REPLACEMENT

Ian S. Roth, Marcel P.J. Gaudreau, Michael A. Kempkes
Diversified Technologies, Inc. Bedford, MA USA

Abstract
Opening switches have substantial advantages over crowbars. Diversified Technologies has developed solid-state opening-switches using series arrays of IGBTs; many systems have been delivered. The control circuitry has been improved, and the current capability of low-cost switches has been increased from 5 to 25 A. The opening switch being developed will be part of a complete klystron power-supply system for the Advanced Photon Source at Argonne National Laboratory.

INTRODUCTION

Crowbars are commonly used to protect klystrons from arc damage. When an arc occurs, the crowbar closes, and rapidly discharges the energy-storage capacitor. A typical crowbar circuit diagram is shown in Figure 1. An alternative way to protect a klystron is to use a switch that opens during an arc (also shown in Figure 1). Opening switches have substantial advantages over crowbars:

- No series resistor is required, so an opening-switch system has higher circuit efficiency.

- Because the energy-storage capacitor does not discharge during an arc, high voltage (and RF) can be turned back on in less than 30 µs, before the circulating accelerator beam dumps [1]; see Figure 2. No beam re-start is required.

- Crowbars use mercury-containing ignitrons. When an ignitron fails, the required clean-up can be time-consuming and costly. As an example, the ignitron failure at the Joint European Tokamak in 1986 shut down the machine for three months. The total cost of the failure, including lost staff time, was £1 M ($1.9 M) [2]. Opening switches use no mercury.

Opening switches can be made using vacuum tubes, but these are expensive, have a large forward voltage drop (10-20% of the total switched voltage), and a limited lifetime. Diversified Technologies has developed opening switches made from a series array of solid-state devices, IGBTs or FETs. These are much less expensive than vacuum tubes, and have much

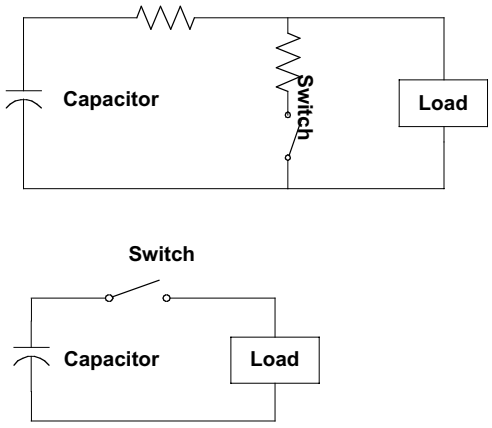

Fig. 1. Circuit diagrams for crowbar (upper) and opening switch (lower).

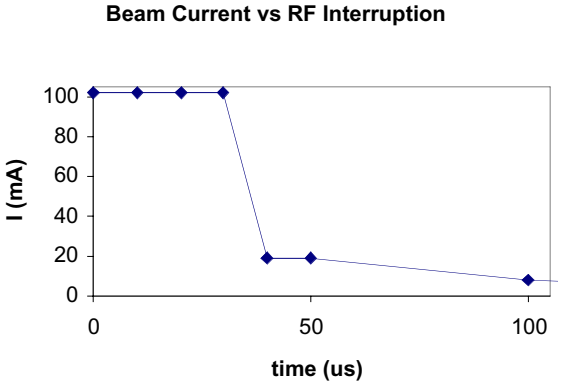

Fig. 2. Beam current vs. RF interruption. An interruption of up to 30 µs can be sustained without beam loss.

longer lifetimes. The forward voltage drop of these opening switches is small, less than 0.5% of the opening switch voltage. Opening switches have been in service for several years without any failures from non-simultaneous opening. An additional benefit of the series-array opening switch is redundancy. Switches are made with excess voltage capability, so the switch can continue operating even if several devices should fail. Diagnostics report any device failures, so repairs can be scheduled appropriately.

OPENING SWITCH OPERATION

An example of an operational opening switch is shown Figure 3 (left). This switch is also used as a modulator, like most of the high-power opening switches delivered. It carries 500 A and opens to

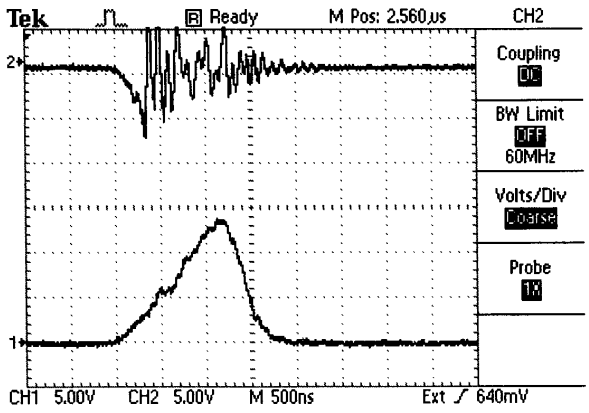

Fig. 3. Left: Opening switch delivered to CPI. Right: Waveforms of a deliberate short. Upper trace, voltage, 50kV/division; lower trace, current, 250 A/division.

140 kV. The unit has been operating at CPI for several years. Waveforms of a deliberate short are shown in Figure 3 (right). The lower trace shows the current. After the current passes the arc-detection threshold of 200 A, it rises for an additional 700 ns before being interrupted. The peak current interrupted is 700 A.

OPENING SWITCH DEVELOPMENT

We are developing opening switches further under a Phase-II SBIR grant from the DOE. There are two directions for the development: improving the control circuitry, and reducing the cost of the specific opening switch.

One of the ways we have developed the control circuitry is to use DC current monitors that have a fast response. In a DC system (often used to drive klystrons) pulsed current transformers do not work well. This is because the ferrite in the transformer saturates, and the transformer will not respond to pulsed fault currents. The pulse response of the LEM DC current monitor (see Figure 4) is fast enough for fault detection.

We have further developed the control circuitry to decrease the system response time to an over-current fault.

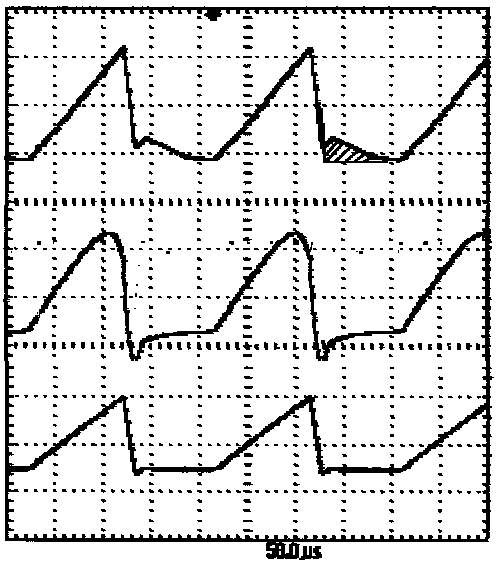

Fig. 4. Identical current waveform with three different diagnostics. Peak current is 30 A; timescale is 50 µs/division. Upper trace, LEM-100P; middle trace: Pearson 110 transformer; lower trace, Pearson 1025 current transformer.

This has been done by using faster fiber-optic receivers (fiber optic cables are used to trigger and diagnose the IGBTs) and increasing the slewing rate of the IGBT trigger. DTI systems presently take 700 ns from the over-current signal to the turn-off of the switch.

We have also added fault latching, which displays the first fault signal, and locks out subsequent signals. This allows the operator to determine the cause of a fault, and make repairs if needed. Finally, we have reduced the number of fiber-optic cables per switch plate from three to two by multiplexing diagnostic signals.

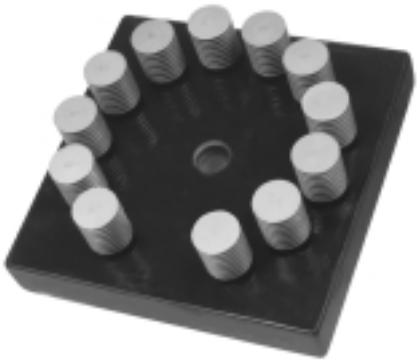

Figure 5. Low-cost switch module**.**

As well as improving the control circuitry, we are increasing the DC capability of low-cost opening switches (Figure 5) from 5 to 25 A. These switches use discrete IGBTs, and are substantially less expensive than ones using IGBT modules. The low-cost opening switch will be incorporated into the klystron power-supply for the Advanced Photon Source (APS) at Argonne National Lab.

To increase the current capability of the low-cost opening switches, we first selected the best IGBT available. The properties of various devices are compared in Table 1.

Table 1 Comparison of discrete IGBTs. $R_{\_JC}$ is the thermal resistance from junction to case; $R_{\_CK}$ is the thermal resistance from case to heat sink.

Device	V_{max} (V)	$I_{max\ DC}$ (A)	$V_{forward}$ (V)	$R_{\_JC}$ (°C/W)	$R_{\_CK}$ (°C/W)	$t_{current\ delay\ off}$ + $t_{current\ fall}$ (ns)
Fairchild HGTG 30N120CN	1200	75	2.1	0.25	0.25	400
IXYS IXLF 19N250A	2500	32	3.2	0.5	0.25	650
IXYS IXGH 45N120	1200	75	2.5	0.42	0.25	760
IR IRG4PH50S	1200	57	1.75	0.64	0.25	2170
IR IRG4PH50U	1200	45	3.20	0.64	0.25	600
APT 50GF120LR	1200	80	2.9	0.32	0.25	430

We chose the Fairchild (formerly Intersil) 30N120CN; it has the lowest thermal resistance and the second-lowest forward voltage drop of the devices available. While the IXYS 19N250A operates at 2500 V instead of 1200 V, the forward voltage drop and thermal resistance of this device are too large to permit operation at the required 20 A DC.

Having selected the IGBT, we investigated heat sinks. The heat sink performance was measured by mounting the sink to an IGBT, lowering the assembly in oil, passing current through the IGBT, and measuring the temperature rise. A selection of the heat sinks we considered is listed in Table 2.

Table 2. Heat sink performance.

No.	Mat'l	Base area (in^2)	Height, fin gap, fin thickness (in)			$R_{\_}$, °C/W still oil	$R_{\_}$, °C/W moderately flowing oil	$R_{\_}$, °C/W rapidly flowing oil
1	Al	0.79	2	0.094	0.063	1.40	0.86	-
3	Al	6.8	1.3	0.25	0.063	0.36	0.21	0.13
5	Cu	6	2.2	0.125	0.063	0.24	0.12	-
9	Al	6.2	1.6	0.19	0.11	-	0.13	-

Heat sink 1, which we have been using, has the highest thermal resistance of the sinks tested. Heat sink 3 was made from extruded aluminum. Note that the thermal resistance was lower when the oil was flowing rapidly (with the device directly at the exhaust of the oil pump) than when the oil was flowing moderately (with the device 18" away from the pump exhaust). We decided, however, that rapidly-flowing oil would be impractical. Heat sink 5 was made from copper. While this heat sink has a low thermal resistance, it was expensive to manufacture, and we decided to use extruded-aluminum heat sinks. Heat sink 9 has a low thermal resistance, 0.13° C/W. Using heat sink 9A, which is made from the same extrusion as heat sink 9 but with half the base area, halves the size of the opening switch while giving only a 7° C increase in temperature. The calculated IGBT-junction temperature rise is then $2.7\ V \times 20\ A \times (0.50 + 0.26)\ °C/W = 41°\ C$.

ARGONNE KLYSTRON POWER-SUPPLY SYSTEM

The opening switch is the first part of a klystron power-supply system we are building for APS. Specifications for the system are listed in Table 3.

Table 3. Specifications for the APS Klystron Power Supply at Argonne.

Component	Specification
Transformer	13.6 kV in, 110 kV out, 2.2 MW
Buck regulator	110 kV in, 0-100 kV out, 20 A out, ±0.5% regulation, >90% efficient
Filament heater	0-25 V, 0-25 A, ±1% current regulation
Mod anode power supply	0-90 kV with respect to cathode, 20 mA
Opening switch	100 kV, 20 A, 1 μs response to fault
Ion pump power supply	3.5 - 5.5 kV, 20 mA
Electromagnet power supplies	0-300 V, 0-12 A, 0.1% current regulation
Controls	interlocks, local/remote operation

In addition to the opening switch, the other potentially difficult component could be the buck regulator. The same technology used for the switch, however, is used for the buck regulator, and the required performance has already been demonstrated: Figure 6 shows a buck regulator that is installed at CPI. This buck regulator gives a power output of 140 kV and 20 A, with regulation to ±0.3%.

The remaining components in the system use conventional technology. We anticipate no difficulty in constructing the complete APS klystron power-supply.

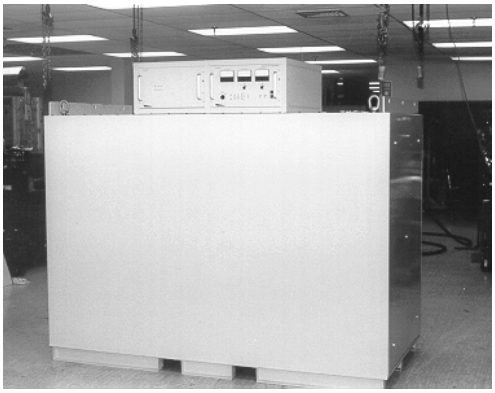

Figure 6. Buck regulator installed at CPI.

REFERENCES

[1] Doug Horan, Advanced Photon Source, Argonne National Laboratory; private communication.
[2] Geoff Pile, Advanced Photon Source, Argonne National Laboratory; private communication.

A THYRATRON FOR THE NLC BASELINE MODULATOR

M. Parmenter, C.A. Pirrie, C.A. Roberts, P. W. Robinson and R. Sheldrake
Marconi Applied Technologies Ltd., Waterhouse Lane, Chelmsford, CM1 2QU, UK.

Abstract
There are several modulator techniques being investigated as candidates for driving NLC klystrons in groups of between two and eight per modulator. The baseline design is a conventional line type modulator that would use a thyratron as the switch to drive two klystrons. This paper describes a thyratron designed to meet these operational requirements. The target lifetime is 50,000 hours. Cost and reliability are of critical importance due to the large number of modulators required. Several design decisions were taken at the outset including cathode type, basic tube diameter and number of high voltage gaps required. The development process included measurement of cathode temperature as a function of average current and electrostatic field analysis of the high voltage geometry. The rationale underpinning the design that resulted is explained. Since the specification was first defined, the pulse width has been doubled with a corresponding doubling of the average current. The impact of this updated requirement on the existing design is also discussed.

1. INTRODUCTION

The table shows the original acceptance test criteria, operational data and the upgraded requirement as a result of the pulse width being doubled. The most significant challenge is to achieve the target life of 50,000 hours; all other parameters have been demonstrated to be well within the capabilities of modern thyratron technology.

Parameter	Original Acceptance Test	Original Operation	Present Operation
Anode voltage (kV)	90	75	75
Peak anode current (kA)	10	7.5	7.5
Inverse voltage (kV)	10 max	not known	not known
Di/dt (kA/us)	100	75	75
Average anode current (A)	2.5	2	4
Pulse duration (70%) (us)	2.2	2.2	4.4
PRF (Hz)	180	180	180
Jitter (ns)	1	1	1
Run time or life (hours)	24	50,000	50,000
Run time or life (shots)	1.55E+07	3.24E+10	3.24E+10

2. KEY DESIGN CONSIDERATIONS AND DESIGN DECISIONS

The work described here builds upon previous work [1,2] where the performance, life and suitability of various thyratron types and designs were discussed. The more recent paper [2] discusses data on the current life history of candidate tubes; it also identifies the optimum means of triggering and considers critical circuit parameters, which need to be considered to maximise thyratron life. These are considered in more detail here.

2.1 Cathode type

The thermionic cathode is one of the key features that will determine the achievable lifetime. The previous work indicates that the barium aluminate (BA) impregnated cathode size used for 4.5 diameter metal envelope tubes (e.g. CX1836 type) and the oxide cathode in the 6 diameter ceramic tubes (e.g. CX2410 type) are the minimum cathode sizes that could achieve 50,000 hours life at 2A average.

Field data supports this conclusion for Marconi Applied Technologies BA cathode tubes [2,3]. Insufficient field lifetime data exists for the Marconi 6 oxide cathode tube at high ($\geq$2A) average current levels, but tubes of this type (CX2410) have been operational at KEK since 1995 at average currents from 0.3 to 1.3A [4]. Recent data from KEK [5] shows that out of the 16 tubes received in 1995 there have been three failures from poor connections to the cathode terminals and that the remaining operational tubes have accumulated an average service life of 17,000 hours to date (with a calculated MTBF of 85,000 hours!). There are lifetime data for thyratrons of this type from other manufacturers that indicate that several tens of thousands of hours are likely to be achieved under similar average current conditions. Since it appears that there is little difference emerging in service life between the BA cathode in the 4.5 tube and the oxide cathode in the 6 tube, the oxide cathode is preferred over the smaller BA counterpart simply on the grounds of cost.

2.2 Reservoir type

A high capacity reservoir system has been selected so that gas pressure adjustments throughout tube life are minimised. The high capacity system is more complex than a conventional reservoir; there are two reservoir capsules which operate at different temperatures and further auxiliary control components to compensate for input power fluctuations and ambient temperature variations. The total gas content, however, is typically more than ten times greater than that of a typical conventional reservoir. This large capacity has the significant added benefit that the need for reservoir ranging to compensate for gas clean-up losses is removed.

2.3 High voltage structure and number of gaps

Previous work [1,2] has indicated that a minimum of three high voltage gaps are required for reliable operation at 75kV under command or resonant charge conditions. Two basic mechanical designs of multi-gap tubes exist as shown in Fig. 1. Fig. 1a is the stackable, repeatable, drift-space structure and Figs.1b and 1c are examples of two and three gap nested-cup structures, respectively. On a parts count and therefore cost point of view, a design like Fig. 1b or 1c is preferred.

2.4 High voltage structure materials

Traditionally, very high voltage structures have been faced with molybdenum because it has proved more resistant to arcing than copper, especially at anode voltages above about 60kV. High voltage structures above this level using copper have been built before but have tended to exhibit destructive arcing. An inherent property of all multi-gap thyratron structures is the very high peak transient electric fields that occur as a consequence of the way the tube commutates. The tube is triggered at the cathode end and the high voltage gaps go into conduction starting with the gap nearest the cathode, followed by a delay of around 50 ns before the next gap, and so on. The result is that the last high voltage gap at the anode must withstand the full anode voltage for a period of around 50 ns without arcing. Molybdenum appears to become electrically conditioned to withstand this (tubes have been operated successfully at up to 160 kV) but copper has been observed to suffer arc damage that prevents this conditioning from occurring. Despite this, copper would be preferred on the grounds of cost and since cost is such an important factor, the design of the high voltage structure was undertaken on this basis. This represented a risk worth taking.

Fig. 2 is a field plot of a simplified representation of the top gap of the proposed prototype design and shows that there is peak electric field of around 13.6 kV/mm when a potential of 30 kV is applied. With an applied anode voltage of 90 kV corresponding to the specification maximum,

these figures are exceeded by a factor of three for a period of 50 nsec or so during commutation. Although the field during commutation is rather high at around 40 kV/mm, it is only a transient field. The limits for acceptable peak field strength under such transient conditions are not precisely known, but test results presented below indicate that they have not been exceeded in this instance. The radii of curvature on the selected geometry are larger than those previously utilised for copper high voltage geometries as a result of the results obtained by undertaking the field plotting work. The generally accepted maximum field strength for d.c. applied voltages in electron tubes with conditioned surfaces is around 10 kV/mm. The field strength in the top gap with 25 kV applied (corresponding to the 75 kV operating level) is around 11 kV/mm, but this field will only be present for a small fraction of a second. The significant magnitude of the transient applied peak fields can be reduced using a relatively simple circuit technique, as discussed next.

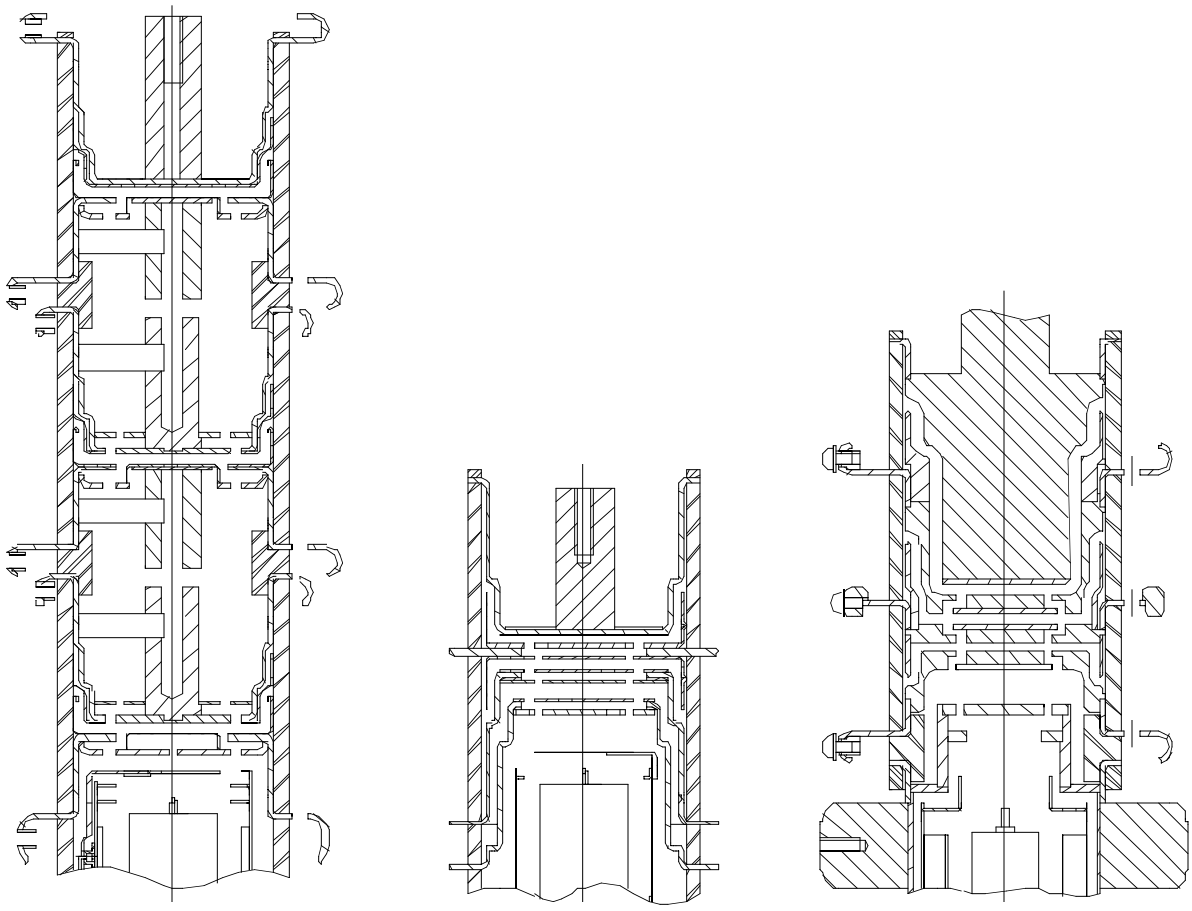

(a) (b) (c)

Fig. 1 Various thyratron high voltage structures. Fig. 1(a) is a typical example of the stackable drift-space multi-gap structure, whilst figs. 1(b) and 1(c) are typical examples of two- and three- gap nested-cup geometries.

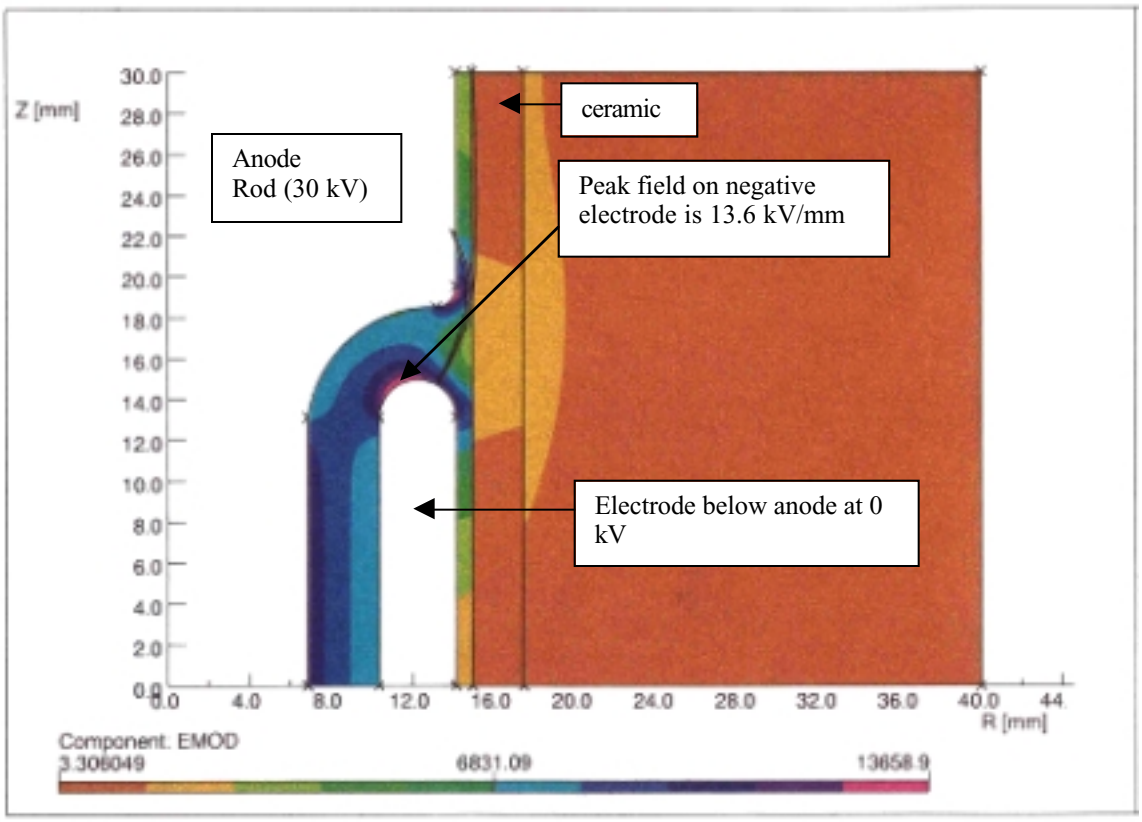

Fig. 2. Electric field plot of the critical area within the proposed top gap geometry. The z-axis represents the axis of the thyratron . Also shown are the trajectories of single electrons released from the surface of the electrode below the anode.

2.5 Saturating anode inductor

To reduce the anode heating arising from switch-on losses, and, more important in the light of the above discussion, to reduce the voltage appearing across the top gap during thyratron commutation, it is proposed to use a saturating anode inductor with this tube design. Detailed work performed at CERN [6] indicates that a saturating anode inductor with a volt-second product of 1.6mVs will give a switch-on delay of approx. 70ns with a three gap of the drift space design and that this will prevent any excess voltage build up across the top gap of such a tube. Shorter delays will offer proportionately less protection and it may be necessary to trade off the effect of the added saturated inductance on the current rise time against the protection afforded to the top gap. Saturating anode inductors also afford some protection against the adverse effects of inverse voltages [7].

3.0 FINAL PROTOTYPE DESIGN

The design that was selected for manufacture is shown in Fig. 3. The key features outlined above are incorporated: an oxide cathode from a 6 diameter thyratron, a high capacity reservoir system, copper electrodes and a nested-cup high voltage structure. The tube envelope surrounding the cathode structure uses copper in preference to the more conventional ceramic and the basic diameter of the control grid and high voltage structures is 4.5 rather than 6 . These features result in a hybrid design that is tailored specifically for this application where cost, reliability and operating lifetime are paramount.

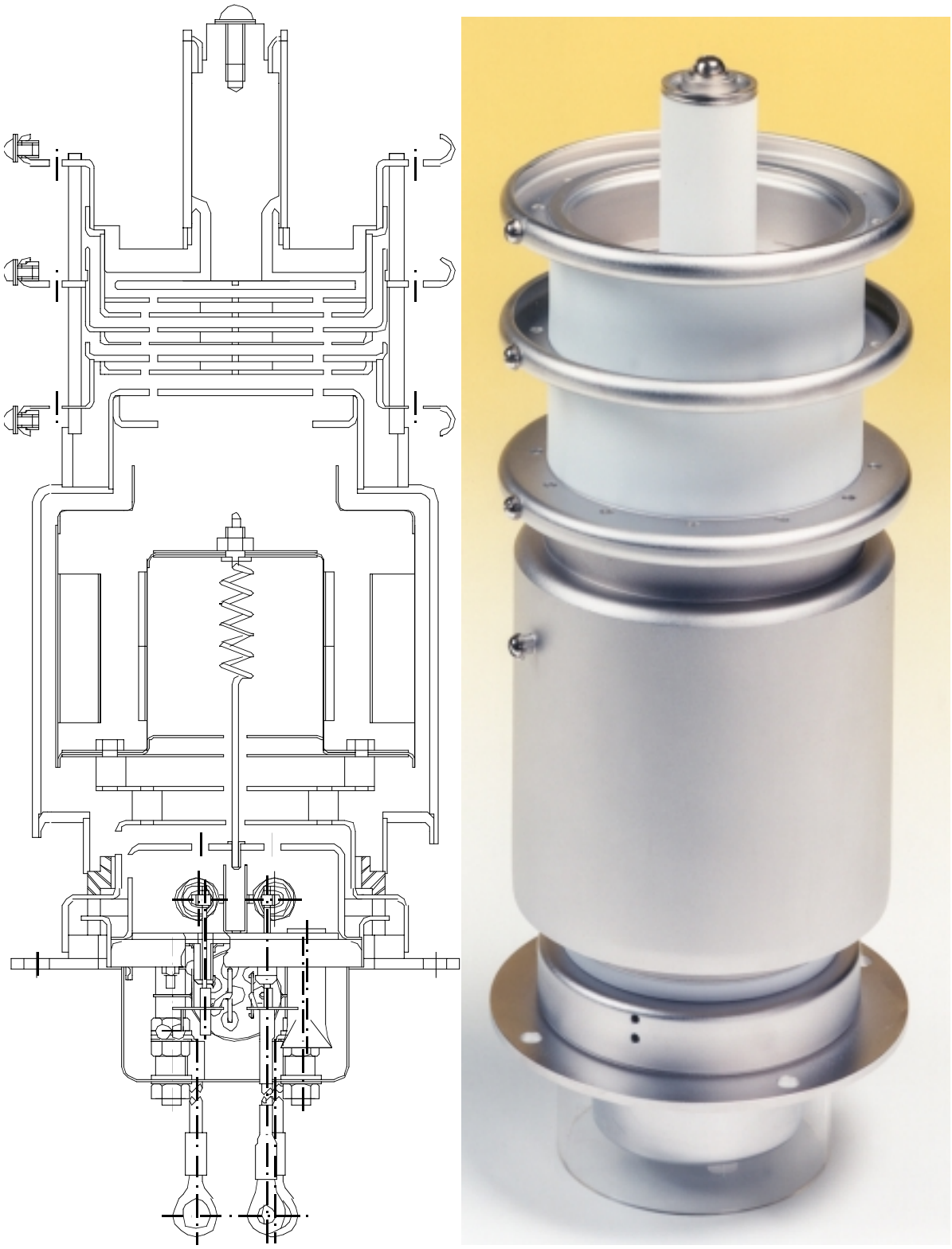

Fig. 3 Drawing and photograph of final CX2437X design for 2A average current operation

4. FACTORY MODULATOR TESTS

4.1 Cathode Temperature Measurement

The optimum cathode operating temperature is a balance between sufficient primary electron emission at one extreme and minimising thermal evaporation at the other. Drawing from experience and published data [8], this temperature lies somewhere in the range 750-780 ^{O}CB. Thyratrons differ from all other electron tubes in that cathode back heating by ion collection/impact will make a significant contribution to overall cathode power dissipation. A sample tube was manufactured with a sidearm window to enable cathode temperature to be measured with an optical pyrometer and fig. 4 shows the measured cathode temperature against average current for the first CX2410 cathode design. It can be seen that the quiescent non-operating cathode temperature is at the top end of the acceptable range and that the temperature climbs significantly as the average current switched is increased (by increasing the prf). Fig. 5 shows how cathode temperature varies with input heater power alone, from which it is deduced that the optimum input power is around 450W to achieve 750 ^{O}CB. This equates to a heater current of 71A at 6.3V and the cathode heater incorporated into the design was selected to have these parameters.

Given that a temperature difference of as little as +25 ^{O}C may double the rate of coating evaporation [9] the importance of getting the temperature correct is evident. Given this, it is perhaps surprising that the practice of operating thyratrons with reduced heater power to compensate for back-heating has not been adopted much more widely. The data in figs. 4 and 5 allow calculation of the required reduction in cathode input heater power to maintain the cathode at the optimum temperature for operation at a given average current.

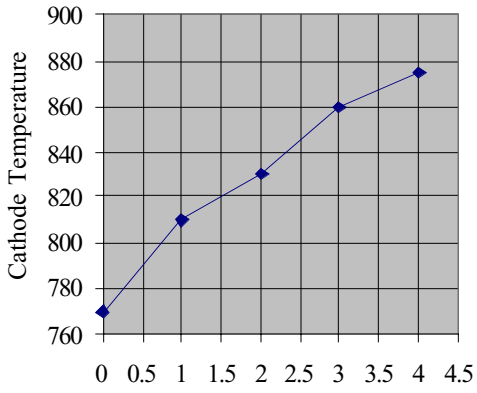

Fig. 4 Cathode Temp. (^{O}CB) vs. Average Current

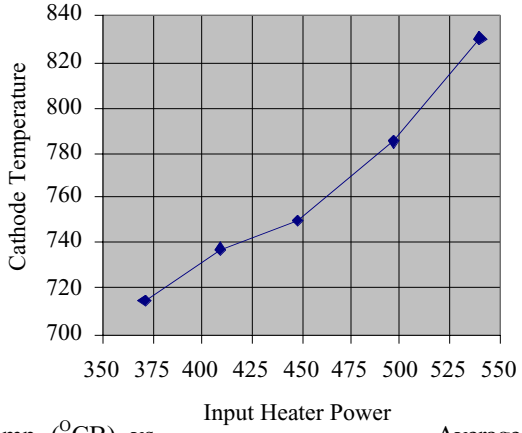

Fig. 5 Cathode Temp. (^{O}CB) vs. Input Heater Power

4.2 High Voltage Operation

Marconi Applied Technologies does not have equipment to test an NLC tube under all conditions simultaneously, but there are separate equipments that can test groups of parameters that collectively encompass most aspects of the specification. The high voltage tests performed on two prototype tubes are summarised below. Both tests were carried out with a saturating inductor giving a switch-on delay of about 18ns (Ferrite type CMD5005, 4 OD, 2 ID, 1 thick) [10].

i) 85kV, 2.83kA, 0.6us pulse in a command charged (2ms with a 8ms hold), fast rate of rise of current (120kA/us) equipment, but at only 5Hz.

ii) 70kV, 10kA, 6us pulse at up to 67Hz (4A average) in a resonant charged, slow rate of rise of current (8kA/us) modulator.

Fig. 6 is an oscillogram of the anode current rise at 85kV with a reasonable gas pressure in the tube: 10-90% risetime, including the overshoot, is 28ns, which gives a di/dt of 101kA/us. Jitter is 0.9ns

peak-to-peak.

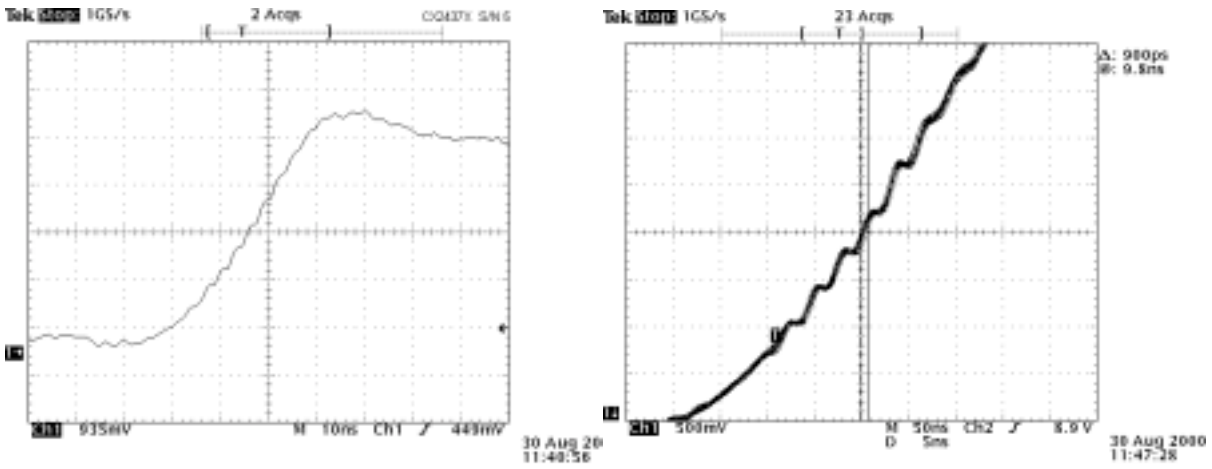

Fig. 6 Anode Current rise-time and Jitter

Under high average current conditions in the 70kV modulator, the two prototype tubes, denoted with type number CX2437, operated flawlessly. One of the parameters measured was the rate of fall of anode voltage, commonly called the dv/dt signal. The dv/dt signal provides a relative measurement of the gas pressure in the high voltage structure. Fig.7 shows the variation of the dv/dt signal as the average current is increased (by increasing the prf) for the two CX2437 tubes. For purposes of comparison, similar data is shown for the CX1536, which is a standard product used commonly in high power linacs of various types. It can be seen that the CX2437 thyratrons display a larger gas pressure variation than the CX1536 as average current is increased. For operation at the 2A average current condition of the original specification, the performance of the CX2437 design is deemed to be well within acceptable limits. The difference between the performance of the CX2437 and the CX1536 is attributed to improved heat extraction from the surface of the anode due to the larger diameter anode rod in the latter. The average cross sectional area of the CX2437 anode rod is only 16% of that of the CX1536.

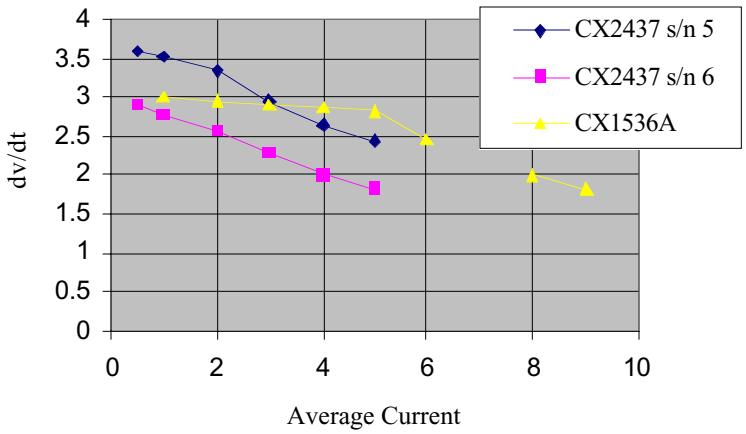

Fig. 7 Dv/dt signal with average current

With a pre-pulse of 10A on the grid 1 and a 0.5us delayed trigger pulse to the control grid 2, CX2437 jitter was around 0.9ns peak-to-peak under both sets operating conditions used in the factory tests and therefore within limits. If needs be, the jitter could be reduced further by using dc power supplies to energise the cathode heaters or by increasing the rate of rise of voltage supplied by the control grid 2 pulse generator.

5. DEVELOPMENTS TO MEET THE LATEST SPECIFICATION

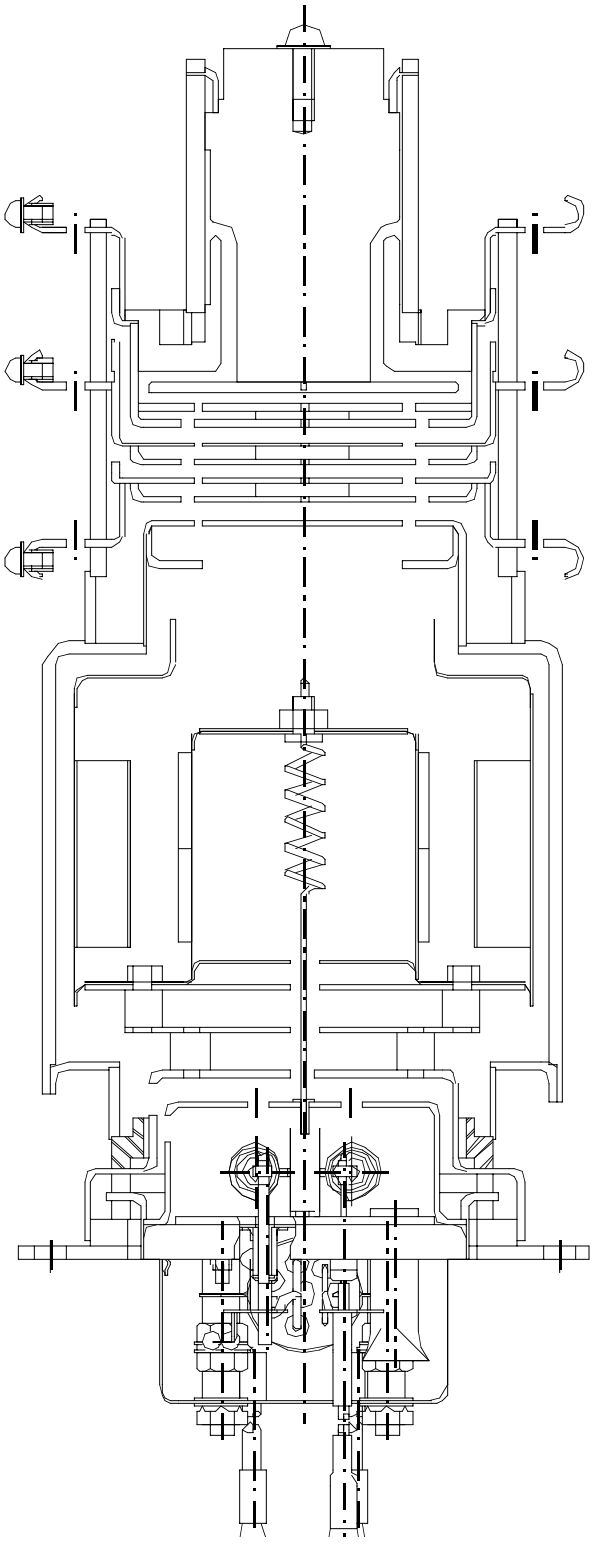

Fig.8 Thyatron design with larger anode.

Fig.7 shows that the doubling of the average current to the 4A level causes a significant fall in the internal gas pressure within the high voltage structure. This can be overcome simply by improving the heat extraction i.e. by incorporating a larger diameter anode rod. Fig. 8 shows a proposed modification where the anode rod has an average diameter approximately four times that of the two prototype samples. It is anticipated that such a tube would exhibit performance similar to that of the CX1536 in fig.7 at up to 4A average current. There is also scope within the existing envelope to incorporate a cathode with a significantly larger surface area, although the figure does not depict this. A larger cathode would be necessary to maintain the 50,000 hours target life in light of the cathode back-heating increasing significantly at double the pulse width.

ACKNOWLEDGEMENTS

The authors wish to thank the directors of Marconi Applied Technologies for permission to publish this paper and to thank those of our customers who have kindly provided life information for this paper.

REFERENCES

[1] R. Sheldrake et al., EEV Thyratrons for NLC Klystron Modulators , Second Klystron-Modulator Workshop, SLAC, 1995. SLAC Report 481 March 1996.

[2] C.A. Pirrie et al. Thyratron and Modulator Design Considerations to Maximise Thyratron Life , 1998 Klystron-Modulator Workshop, SLAC, 1998.

[3] Private communications on life information for CX1836A and CX2412A types.

[4] M. Akemoto et al., Thyratron Performance in the KEK 8 GeV Linac , 25th Linear Accelerator Meeting. SPring-8, July 2000.

[5]Private Communication KEK, May 2000.

[6] L. Ducimetiere & D. Fiander, Commutation Losses of a Multigap High Voltage Thyratron , IEEE 19th Power Modulator Symposium 1990.

[7] C.A. Pirrie et al. Thyratron Design and Circuit Techniques to Overcome the Adverse Effects of High Inverse Voltages , 21st International Power Modulator Symposium, Los Angeles, 1994. (Also EEV Technical Reprint 195).

[8] Research Study on Hydrogen Thyratrons , EG&G Inc, in three volumes as follows:
Volume 1, S.T.Martin, S.Goldberg, 1953.
Volume 2, S.Goldberg, 1956.
Volume 3, S.Goldberg, D.F.Riley, 1957.

[9] S.Goldberg, Cathode Phenomena and Life in Hydrogen Thyratrons , Proc. Seventh Symp. on Thyratrons and Modulators, pp5-9, 1962.

[10] Ceramic Magnetics Inc., published data. http://www.cmi-ferrite.com

HIGH VOLTAGE, HIGH CURRENT, HIGH DI/DT SOLID STATE SWITCH

Steven C. Glidden
Applied Pulsed Power, Inc.
Box 1020, 207 Langmuir Lab, 95 Brown Road, Ithaca, New York, 14850-1257
tel: 607.257.1971, fax: 607.257.5304, email: app@epix.net

Abstract

A high voltage, high di/dt, modular solid state switch intended to replace thyratrons in high power modular applications is under development. This paper describes results of testing a switch module with a 10kV, 6kA, 30 kA/μs, 3μs PFN, under normal and load fault conditions. Initial results of multiple module tests with a 30kV PFN are also be presented. The switch module uses 3, 5kV, 13mm diameter thyristors connected in series. These thyristors were developed specifically for pulsed power applications, and have an interdigitated gate/cathode geometry to minimize turn-on losses and maximize di/dt. The module's trigger circuit uses the switched energy to drive the thyristor gates, eliminating the need for an external gate drive power supply. A 35V, 1A, pulse triggers the module. The compact, modular package design facilitates the development of drop-in replacement switches for thyratrons with voltage ratings of >60 kV.

Work supported by U.S. Department of Energy, grant DE-FG02-00ER82948.

INTRODUCTION

The goal of this project was to demonstrate the feasibility of developing a compact, high voltage, high power solid-state switch based upon newly developed thyristors. The switches consist of multiple 10 kV modules connected in series to achieve the desired voltage rating. The switches are intended to replace thyratrons and other high current, high voltage switches in existing and new systems. The small size of the solid-state modules will enable the switches to fit within a volume similar to the thyratrons they are replacing.

The 10 kV switch modules consist of a series array of 3 thyristors with built-in trigger circuitry. The trigger circuit uses the energy being switched to drive the thyristor gates, simplifying isolation and triggering. The elimination of the need for a separate gate drive power supply results in a straightforward process of scaling to higher voltages. The thyristors are capable of high di/dt operation without saturable inductors.

This work has shown that a 10 kV module can operate reliably at currents up to 8 kA at di/dt's of > 30 kA/μs. The di/dt was limited by the test circuit; di/dt's of up to 80 kA/μs have been observed in single devices. Repetition rate operation at up to 60 pps, limited by the high voltage power supply, was demonstrated. Also it was shown that load faults, whether occurring at the beginning or middle of the pulse, did not damage the thyristors when there is some damping in the circuit. Tests at 30 kV with three modules connected in series, showed simultaneous turn-on with good voltage-sharing between modules.

10 kV MODULE DESCRIPTION

The 10 kV switch module consists of 3 symmetric (reverse blocking), 5 kV, 13 mm diameter thyristors connected in series. No attempt was made to match thyristor characteristics other

the energy being switched to drive the thyristor's gate. A 35 V, 1 A, 50 ns risetime pulse triggers all three gate circuits. Each trigger transformer was hi-potted to 60 kV. All of the 10 kV module components are mounted on an 11 x 16 cm circuit board.

The 13 mm diameter thyristors[1,2] used for the switch have been developed specifically for pulsed power applications. These devices have an extensive, serpentine gate pattern that is everywhere less than one diffusion length from the cathode, and a heavy gate connection which allows > 1 kA gate current to minimize turn-on losses and maximize di/dt. A solid metal cathode structure efficiently collects charge during conduction, eliminating excess current density and hot spots. The device has an active area of 0.1 cm^2. The positive beveling at the edge of the thyristor die acts to spread out the electric field lines on both sides of the high voltage junction when the device is forward biased.

The thyristor is packaged in a 26 mm square package. The anode side of the silicon chip is soldered to a metalized layer deposited on a BeO ceramic base. Wire-bonded cathode leads add approximately 8 nH of cathode inductance. As a result, the gate-cathode voltage rises dramatically during high di/dt turn-on.

The BeO insulator that is part of the thyristor package, will hold off only 5 kV and the heat sink is typically held at ground potential. A second layer of ceramic between the device and the heat sink provides additional voltage insulation. One mm thick AlN ceramic was used for this purpose. Several different interface materials were placed between the ceramic layers and the heat sink to improve thermal performance. For the repetition rate tests, the copper heat sinks were mounted to a water-cooled chill plate that was maintained at 22 degrees C.

Gate drive circuits using MOSFET's, IGBT's or thyristors to switch a portion ot the energy from the snubber capacitors into the thyristor gates were tested. Figure 1 shows the gate drive currents of the three thyristors for a typical pulse with a MOSFET gate switch. The abrupt decrease in gate current occurs because of the large inductive voltage drop across the cathode during turn-on, reducing the effective gate drive voltage. Experiments showed that an increase in the gate current from 60 A to 110 A decreased the total turn-on delay by 20 ns.

OPERATION WITH A NOMINAL 3 μs, 6 kA PFN

Figure 2 shows typical performance using the switch to discharge a 1.68 μF, nominal 6 kA, 3 μs PFN charged to 10.4 kV into a 0.7 Ω load. Two switch voltage waveforms are shown. The first is the voltage as measured by a 1000:1 high voltage probe, and the second (bold) waveform is this voltage minus the L di/dt inductive voltage drop across the switch. This second waveform is used to determine the energy deposited in the switch during turn-on, and for comparisons of switch turn-on at different currents. The maximum di/dt of 27 kA/μs is limited by the circuit.

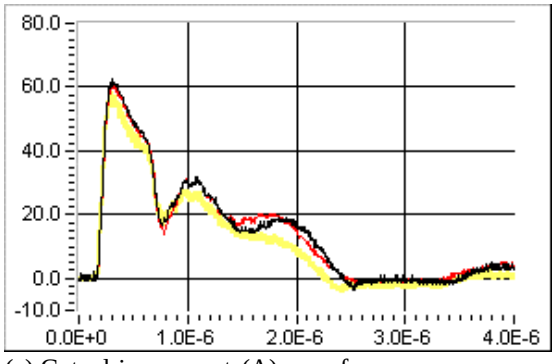

(a) Gate drive currents(A) waveforms.

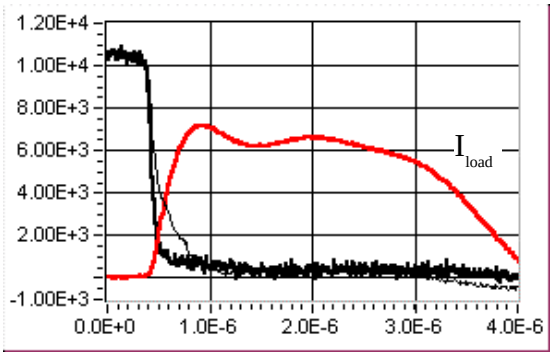

(b) Switch voltage(V) and load current(A)

Figure 1 Typical switch performance with a 1.68 μF PFN charged to 10.4kV.

TURN-ON DELAY AS A FUNCTION OF VOLTAGE AND CURRENT

The module's turn-on delay and voltage falltime as a function of current were observed by using the three different PFNs (0.56, 1.12 and1.68 μF, nominal 3 μs pulsewidth) charged to the same voltage. As indicated in Figure 2, these times are unaffected by the circuit impedance over the range from 0.88 to 2.6 ohms.

The module turn-on delay time is a strong function of the voltage across the module. To a lesser extent, the voltage falltime also increases as the voltage decreases. Data taken with the 6 kA PFN at several different voltages is compared in Figure 3. Operation at module voltages below about 3 kV is undesirable, as the voltage falltime begins to increase.

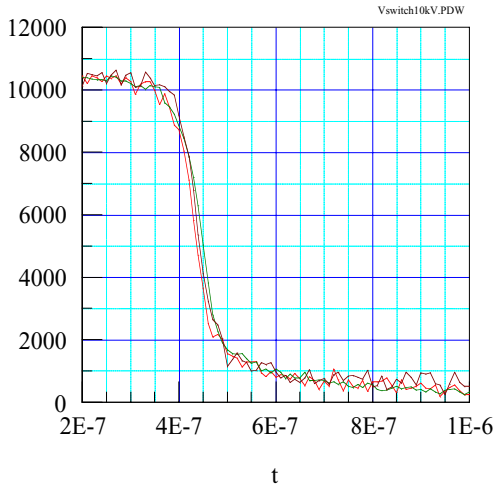

Figure 2. Effects of switch current on turn-on delay and voltage falltime for nominal 2kA, 4 kA and 6kA PFN's.

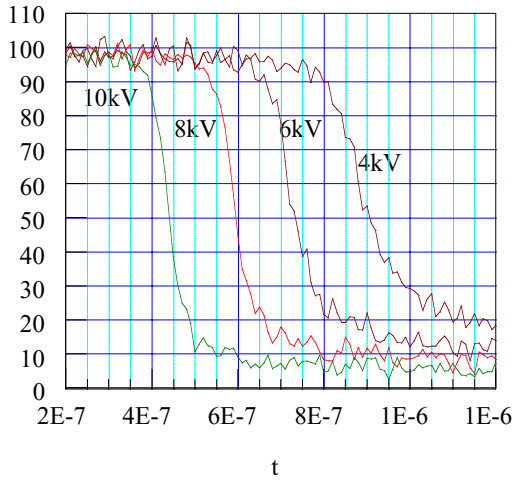

Figure 3. Effects of switch voltage on turn-on delay and voltage falltime with 1.68μF PFN

Turn-on delay is partially caused by the time required for minority charges (electrons) to transit the p base of the thyristors. Field-aided drift theory states that this time can be reduced by a high electric field, which increases the drift velocity of minority carriers across the bases, and thereby speeds up the turn-on. If the field is small, the charge transits by diffusion or W2/2D, where W is base width and D is the diffusion constant. If a high field is present, than transit velocity is increased proportional to electric field.

Similarly, high di/dt current, from either the snubber capacitors or the external circuit can speed the later stages of turn-on. The high current generates a large electric field in the wide n- base, increasing the velocity of the holes crossing it.

VOLTAGE SHARING

Figure 4 shows the dynamic voltage sharing between the three thyristors in a 10 kV module. All three devices turn on together. In Figure 5, a shunt resistor has been added across one thyristor to deliberately produce a mismatch in the DC voltage. As a result, this thyristor has a longer turn-on delay. Nevertheless, none of the devices see excessive voltage during turn-on. The field-aided turn-on mechanism helps to insure that any thyristor initially bearing a greater percentage of the module voltage, due perhaps to changes in leakage current as the devices heat up, will always be the first to turn-on and thus not see additional voltage.

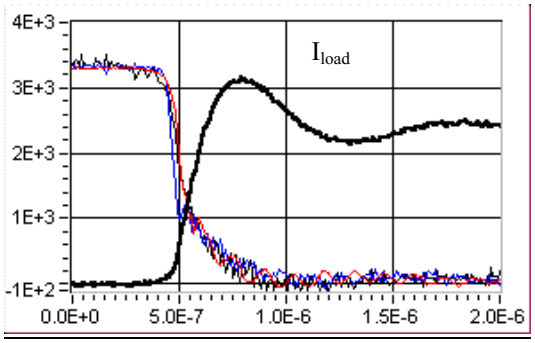

Figure 4. Voltage across each thyristor with compensation for loading by high voltage probes. PFN voltage is 10.0kV.

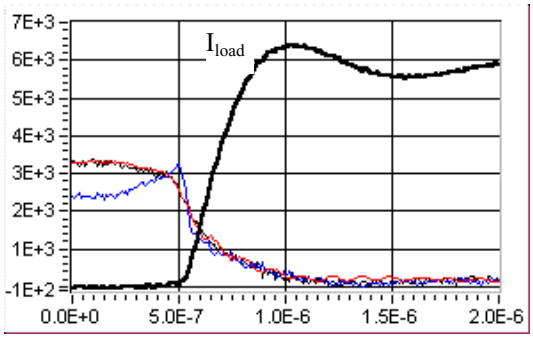

Figure 5. Voltage across each thyristor with deliberate mismatch for 1 device. PFN voltage is 9.0kV.

REPETITION RATE OPERATION, THERMAL PERFORMANCE

The PFN was charged by a 1 kJ/s capacitor charging power supply gated off for 25 μs during switching. Repetition rate testing was limited by the capacity of the power supply. Tests were performed at ≤ 60 pps, 1.9 kA peak and 23 A_{rms} with the 0.56 μF PFN; and at repetition rates of ≤ 24 pps, 4.6 kA peak and 35 A_{rms} with the 1.68 μF PFN. With this PFN operating at 35 A_{rms} , a 27 C temperature difference from thyristor to heat sink was measured.

The thermal resistance of a the thyristor is 0.5 C/W to the bottom side of the BeO ceramic. The additional ceramic layer needed for 10 kV insulation results in a ceramic-to-ceramic interface and a ceramic-to-metal heat sink interface. Several different interface materials were tested. A one part viscous, nonconductive epoxy, loaded with AlN powder, was used for most of the testing. This resulted in additional 0.6 C/W thermal resistance, due primarily to the thermal resistance at the interfaces, which was much higher than expected. Examination of the epoxy layers after testing show they were thicker than intended (0.13 to 0.16 mm instead of 0.05 mm) and there were a large number of voids throughout the epoxy. It should be possible to obtain substantially better results. A high-conductivity thermal grease with a viscosity similar to the epoxy was also used, requiring a clamping mechanism to hold the thyristor/ceramic sandwich on the heat sink. We had better thermal performance with this arrangement. Unfortunately, the grease tended to flow out towards the edge of the ceramic, even after several days. Because the grease is a poor insulator, breakdowns occurred around the edge of the insulating ceramic, destroying the thyristor at the high voltage end of the module.

FAULT MODE PERFORMANCE

Experiments were conducted to examine the behavior of the switch under load fault conditions. To simulate a load fault, a spark gap was placed across the load resistors. The gap was adjusted to cause breakdown to occur during both the early and middle stages of the pulse. Because the thyristors used in the switch are not intended to conduct current in the reverse direction, a stack of three 5 kV diodes were connected in parallel with the switch. Initially, there was no damping in the circuit other than the switch resistance.

Initial tests were performed using the switch to discharge a 1.68μF, 8 μs PFN charged to 10 kV into a 2.2 ohm load. Figure 6 shows the results of breakdown of the load during the pulse. When a fault occurs, there is substantial reverse current conduction through the switch as the diode stack begins to conduct current. The peak current on the second positive half-cycle is approximately 95% of the initial. Also, there is no gate drive during the second and succeeding forward current cycles. The switch withstood many pulses of both early and late time breakdown of the load, at < 1 pps repetition rate using this PFN, without failure.

The same switch was then used with the nominal 6 kA, 3µs, 1.68µF PFN. A much higher current and di/dt results for the same PFN energy as in previous tests. Figure 7 shows switch performance with the PFN charged to 6.5 kV for early load breakdown. Again, there is substantial reverse current conduction through the switch before it turns off, and there is no gate drive during the second and succeeding forward current cycles.

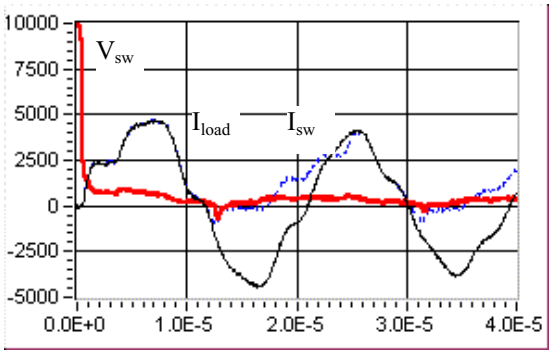

Figure 6. Load fault, 8µs PFN. Switch voltage, V, (bold), load current, A, and switch current, A, (dashed).

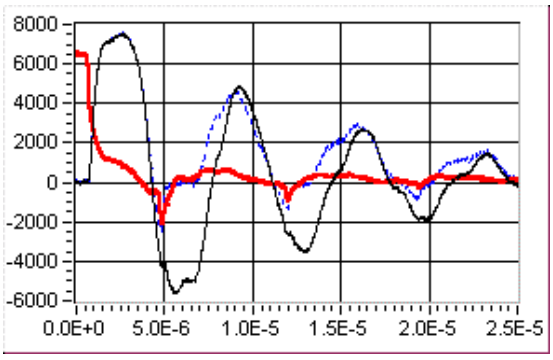

Figure 7. Load fault, 3µs PFN. Switch voltage, V, (bold), load current, A, and switch current, A, (dashed)

After approximately 15 pulses at 6.5 kV, one of the three thyristors failed. Several pulses later, the remaining devices were destroyed. The waveforms for this pulse are shown in Figure 8. Careful examination of the switch current waveform shows that the switch stopped blocking reverse current during the third cycle. This indicates the devices were not destroyed by the initial over-current, but were instead destroyed during one of the succeeding forward current cycles, when the thyristors were forced to conduct current at high di/dt with no gate drive applied.

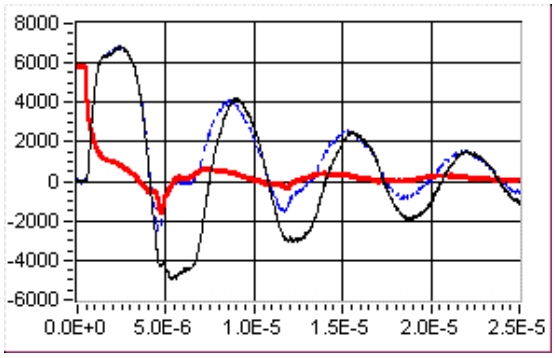

Figure 8. Load fault with switch failure.

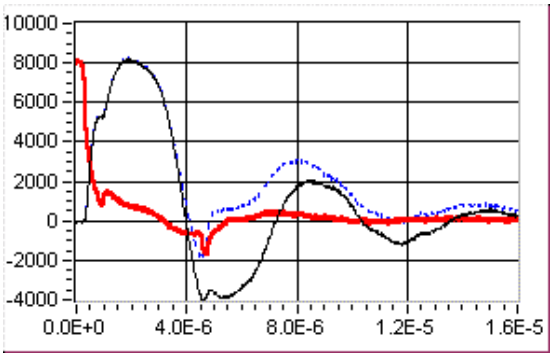

Figure 9. Load fault, 3µs PFN.

Switch voltage, V, (bold), load current, A, and switch current, A, (dashed); both figures.

Additional load fault experiments were conducted with a 0.2 ohm damping resistor in series with the spark gap. With this resistance in place, the initial current reversal was limited to 50 percent. Operation for many pulses at fault currents > 8 kA caused no damage to the switch. Figure 9 shows switch performance with the PFN charged to 8 kV and breakdown in the middle of the load pulse.

MULTI-MODULE TESTING

Some experiments were performed using 2 and 3 modules connected in series, to switch a nominal 4µs, 5-section, type E pulse-forming network with a total capacitance of 0.75 µF. The PFN and switch assembly were installed in a small tank to allow back-filling with $SF_{6,}$

for future operation at up to 50 kV. The load consisted of several bulk ceramic resistors connected in parallel for a combined resistance of ≈ 2 ohms.

Figure 10 shows a result of a 3-module switch operating at 30 kV and 7 kA. Peak di/dt is approximately 20 kA/μs. Because only three high voltage probes were available, one of which is used to monitor the load voltage, the voltage across each individual stage could not be monitored. The voltage across the switch and the voltage at one of the junctions between two modules was measured. Thus, figure 10b shows a comparison between the voltage across one stage and _ of the voltage across the other two stages. The excellent dynamic voltage-sharing shown in this figure was observed regardless of which module was monitored. For these measurements, resistors were placed across the appropriate modules to compensate for the probe resistance.

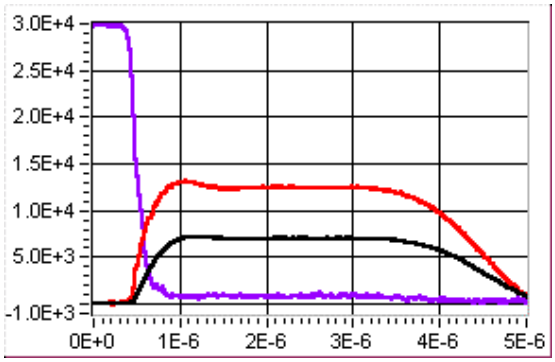

(a) Switch Voltage (V) after subtracting inductive voltage drop, load voltage(V), and load current (A).

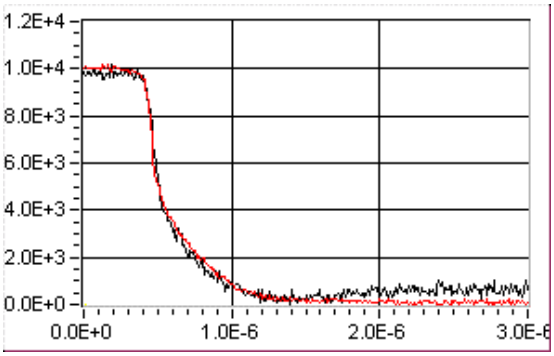

(b) Voltage (without subtracting inductive voltage drop) across modules 3 (lower) and 0.5 times the voltage across modules 1 and 2.

Figure 10. Three module switch charged to 30 kV.

SUMMARY

This work has demonstrated that a 10 kV module can operate reliably at currents up to 8 kA with di/dt's of > 30 kA/μs, and can withstand severe load faults. Repetition rates of up to 60 pps, limited by the high voltage power supply were demonstrated. Tests at 30 kV with three modules connected in series, showed simultaneous turn-on with good voltage-sharing between modules.

Future effort will concentrate on improving the thermal performance of the switch to increase its power handling capability and minimize thermal fatigue. A new asymmetric (reverse conducting) thyristor package design will be implemented to minimize cathode inductance, reduce thermal impedance and eliminate the need for two layers of ceramic. The gate circuit will be modified to provide current over a longer time to improve the fault tolerance of the switch. A prototype 60 kV switch that can be installed into a modulator in place of a hydrogen thyratron will be developed.

REFERENCES

1. J. C. Driscoll et al., "A High Speed Pulser Thyristor", Proceeding of the 1998 Applied Power Electronics Conference, Anaheim, California, Feb. 15-19, 1998.

2. J. C. Driscoll et al., U.S. Patent No. 5,592,118 Jan. 07,1997.

SEMICONDUCTOR SWITCHES REPLACE THYRATRONS AND IGNITRONS

A. Welleman, E. Ramezani, U. Schlapbach
ABB Semiconductors AG, CH-5600 Lenzburg, Switzerland

Abstract
A solid state switching system is presented which is designed a high reliable, long life, low maintenance product for short repetitive and high di/dt pulses. The solid state switch uses special designed semiconductor devices with integrated fast triggering circuits which are powered by one closed loop current source power supply. Blocking voltages of over 30 kV are possible by stacking several devices in series connection. The solid state system has no environmental restrictions and can be used in any position

1) INTRODUCTION

Since several years ABB is offering complete solid state switches which are based on a wide range of specific devices which are designed for non-repetitive pulsed power applications. More recently, interest has been shown in fast semiconductor switches which can be used at medium frequencies, to replace thyratrons and ignitrons because of longer life, no use of mercury and almost no maintenance. For this applications, ABB has designed a new platform technology and is using this concept in a range of different switches. These switches are so called Power Parts, as they are built up as an assembly with semiconductors, drivers, clamping, cooling, power supply and triggering, but are without cabinet or control system.

2) SEMICONDUCTOR DEVICES

The evolution of silicon wafers for high di/dt application started about 1975 with the central gate SCR's capable to handle 200 – 400 A/µs, followed later by higher interdigitated gate structures which allowed about to double these values. Since 1992 the use of GTO-like structures has improved the di/dt handling tremendous, but only in combination with special buffer layers and very low electron-irradiation, it was possible to develop an acceptable wafer for high current, high di/dt and repetitive switching. To reduce the inductance between switch component and freewheeling diode, the last one was directly integrated on the same silicon wafer. A GTO-like wafer structure with integrated freewheeling diode is shown in Fig. 1 (right) direct next to a full switching wafer without diode.

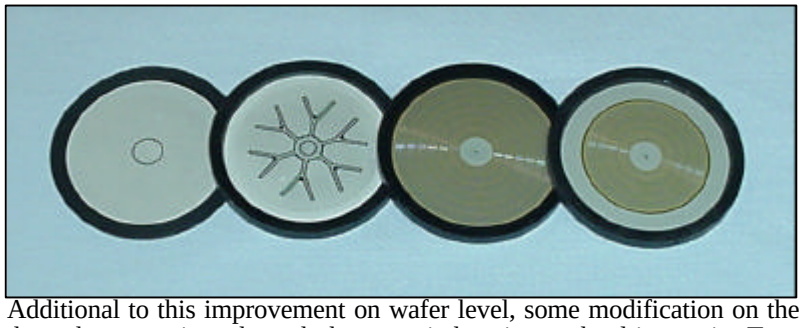

Additional to this improvement on wafer level, some modification on the device housing was done to get more through-connections through the ceramic housing to the driver unit. To get the shortest possible low inductance distance to the driver unit, the driver was built-up and integrated around the ceramic semiconductor housing. With this solution the inductance between switch, freewheeling diode and the driver unit can be reduced to only a few nH. This compact component is the base of a platform technology where a family of 3 different sizes (51 / 68 and 91 mm O.D.) can be used to design switch-assemblies for different current levels and thermal requirements. For Thyratron or Ignitron replacement normally a Reverse Conduction device will be used, but Reverse Blocking or Asymmetric versions are also available. The standard blocking voltage is rated at Vdrm = 4,5 kV and max. cont. DC Voltage is 2.8 kV, or 3.6 kV < 1 min. The switching system presented is using a 51 mm reverse conducting semiconductor discharge switch with integrated driver unit, ABB P/N 5SPR 08F4500. See Fig. 2 and Fig. 3.

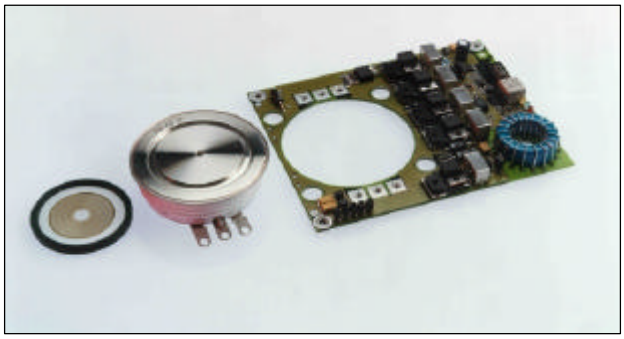

Fig. 2) Reverse conducting 51 mm discharge switch showing wafer, switching device and driver unit separated.

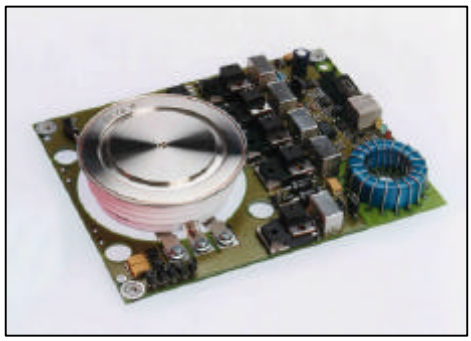

Fig. 3) Device 5SPR 08F4500 complete

The device 5SPR 08F4500 can be used within a wide specification, of which the key parameters like pulse current, pulse length, rep. rate and cooling are the main factors to make a reliable design. The basic specification of the device is Vdrm = 4.5 kV / Vdc max = 3.0 kV / di/dt = 10 kA/µs / peak-pulse current = 10 kA @ tp = 50 µs / Rep.rate ≤ 400 Hz.

3) DRIVER UNIT, INTEGRATED WITH 51 mm DEVICE

To reach a very low inductance the driver unit is integrated direct around the semiconductor switching device. With this construction , and the very low induction gate-connection path, high di/dt and very fast switch-on can be reached. As the switching component is designed for repetitive use, the driver unit has an on-board power supply, which needs an external power source. In case of one single device, the isolation can be easily handled, but in case of stacking several devices in series connection, galvanic separation between the driver units is getting dominant. Therefore it was decided to equip the driver unit with an input transformer, using inductive extraction fed by a separate current source. The current source operates with a 25 kHz closed loop, using an HV-cable, which is sloped through the input transformers of all the driver units. The triggering of the switch is activated by an optical signal. The optical receiver in the driver unit is a commercial HP optical receiver for glassfibers. The driver unit accommodates LED's which indicate Status, Power and Faillure mode. The power consumption of the driver unit is depending on switching frequency, which is about 4 W for up to 50 Hz and 10 W for 400 Hz.

4) POWER SUPPLY

A closed loop current source power supply is used to energize the driver units. In standard version this is done with 25kHz / 4 A, using a closed loop high voltage cable sloped through the input transformers of the driver units. The HV-cable has an isolation voltage of over 30 kVdc cont. Therefore the series connection of devices can easily go up to a charging voltage of 25 kVdc, which means about 10 device switching levels. For higher voltages, a master – slave combination of power supplies, or isolation transformers to feed more power supplies has to be used, and series connection of stacks has to be provided. Fig. 4 shows the power supply for the 51 mm devices.

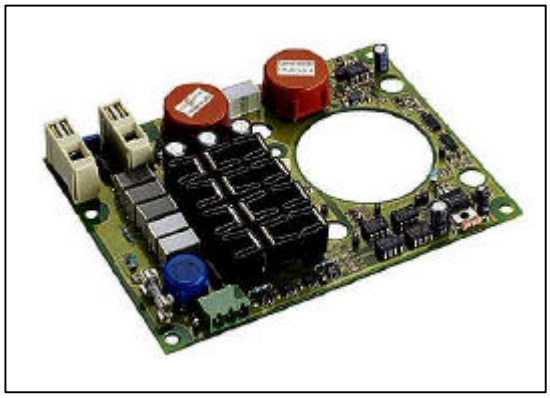

Fig. 4) Current Source Power Supply

5) LIGHT EMITTER BOX

The driver units of the switches are activated by optical signals, which are provided by a light emitter box (Fig. 6). For simultaneous triggering of all devices, the light emitter box has the same amount of optical output sockets as the switch assembly has devices in series connection. In addition there is one optical output to monitor the function of the box. The trigger signal provided to the box can be electrical or optical, depending on system requirements. It is recommended to use optical input for the trigger signal to avoid any interference by high electric fields in the switch area. Therefore it is also recommended to use the light emitter box away from the switch assembly. The pulse-length of the trigger signal is an extreme important value, as the switch needs to be on during the full time of the main pulse. This means that if the main pulse, incl. ev. negative parts, is total f.e. 20 µs, the trigger pulse should be at least 30 µs long, and stopped only shortly before recharging will start again.
This is also shown in Fig. 5. The test was done over 6 device levels (15 kV) and a 12 kA pulse peak.

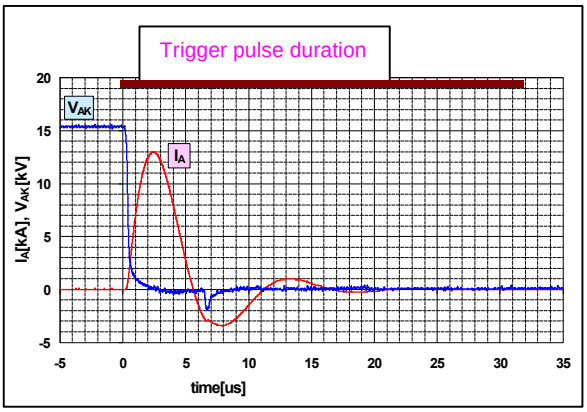

Fig. 5) Example for trigger pulse duration vs. main pulse

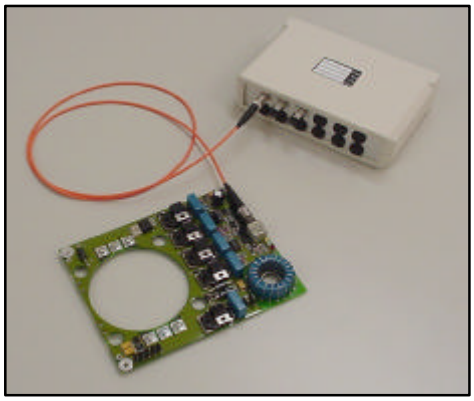

Fig. 6) Light distribution box with optical cable and driver unit

6) THYRATRON REPLACEMENT

Based on the circuit diagram for thyratron with freewheeling diode, ABB has designed a switch assembly, which offers the same performance, but is superior in handling, maintenance and lifetime expectancy.

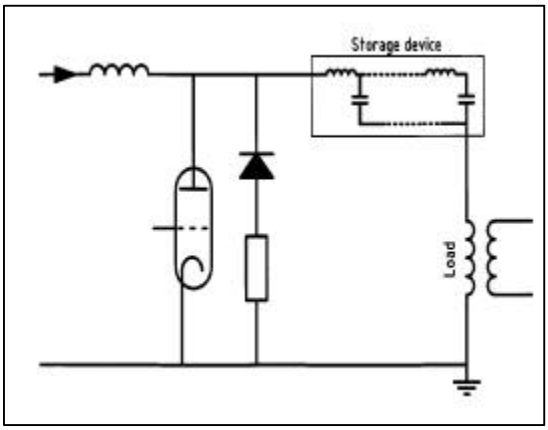

Fig. 7) Circuit diagram thyratron switch

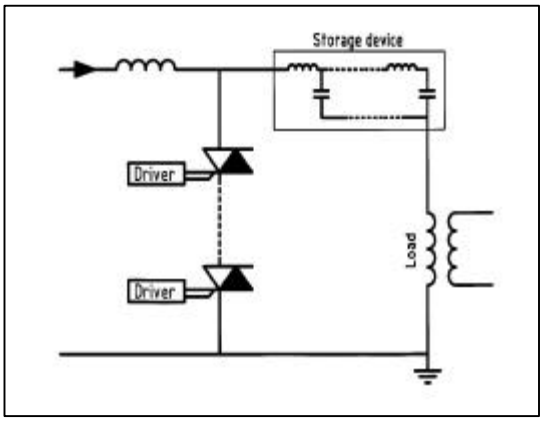

Fig. 8) Circuit diagram solid state switch

7) SOLID STATE SWITCH ASSEMBLY

The solid state switch assembly was designed for 12 kVdc charge voltage, using reverse conducting devices and typical specified for I-peak = 1,5 kA / di/dt = 1,5 kA/µs / tp = 10 µs and a rep. rate of 300 - 400 Hz. For this a

series connection of 6 devices is used, which results in a Vdc of 2,0 kV per level. By using only 2 kV per level it is possible to keep the sharing resistors at a moderate level and cosmic ray has no influence on the life-time of the devices. There is also at least one redundant device in the assembly in case of device faillure. Depending on ambient temperature and cooling capability in the system it is possible to operate the assembly with deionized water cooling or forced air blowing to the assembly. The right cooling method depends on the application condition and can be calculated. Larger systems, with larger semiconductor devices, offering higher currents but based on the same principle are available, but are not part of this paper.

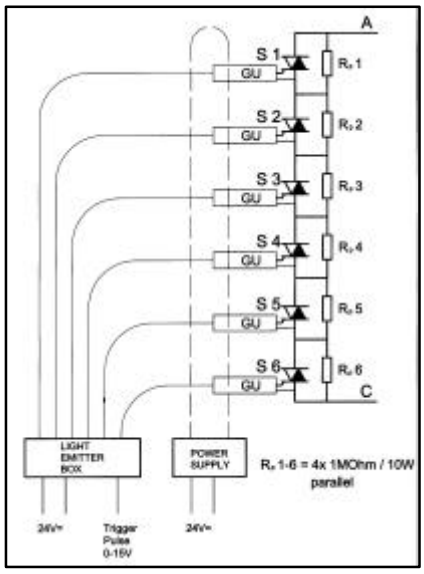

Fig. 9) Basic circuit diagram of solid state assembly.

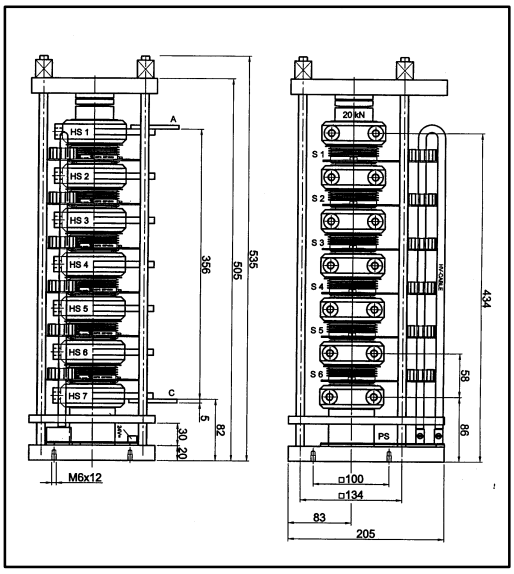

Fig. 10) Design drawing of solid state assembly.

The described switch is using standard ABB water-cooled heatsinks with 60 mm contact area. These heatsinks have two functions, one is the cooling of the devices at higher rep.rates, and second is the spacing between the driver units, giving enough isolation distance to avoid flash-over if used in air. The clamping system is built-up with fiberglass epoxy (Vetresit) parts and rods for good isolation and eliminating inductive heat-up. A 20 kN pressure pack with Belleville springs assure the clamping. In Fig. 11 the complete 6-level switch assembly is shown, including the power supply at the bottom of the assembly. The Light Emitter Box with optical cable to each driver board is shown at the top side of the stack assembly, but it is recommended to move this box away from the assembly to avoid any interference coming from the system or surrounding parts. Tests have shown that the delay time of the total solid state switch is typical less than 600 ns, and the Δ td between the different driver units is less than 50 ns.

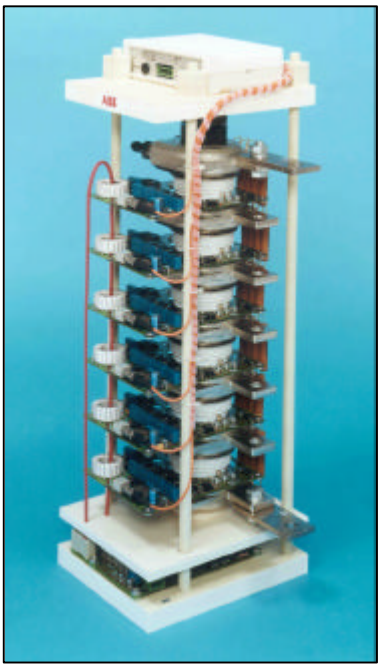

Fig. 11) Solid State Switch Assembly EFM-SPR 08F4500-6-WC

Vdc:	12 kV
I-pulse:	1,5 kA
tp:	10 µs
di/dt:	1,5 kA/µs
f:	400 Hz
Devices:	6 x 5SPR 08F4500 in series connection
Cooling:	Deionized water
Supply:	24 Vdc
Trigger:	Optical input

8) TEST RESULTS

Extensive testing is done on wafer, device and driver unit level, this includes the standard factory routine testing. Beside the component test the switch assembly is functionally tested per device level and as full assembly as such. This includes also recording of the data, as far as possible oriented to the customer application. The presented switch assembly was designed for an application to replace a thyratron tube with the given data. As shown in Fig. 5, the assembly is capable to reach different values, like higher peak current and shorter or longer pulse widths. Fig. 12 is showing a test result with a 1,5 kA pulse measured over one device level (2 kVdc) and the related trigger pulse duration.

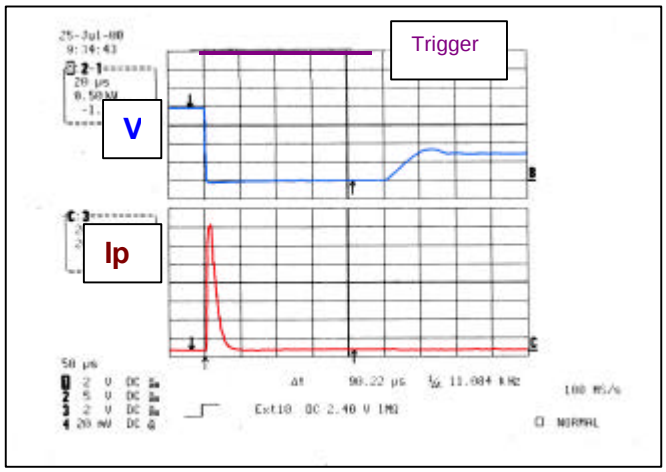

Fig. 12)
Test result over one device level
51 mm device P/N 5SPR 08F4500

The presented devices, drivers units, power supplies, heatsinks and complete switches are available since the end of 1999 with moderate delivery times of about 8 weeks. Because of using a modular platform technology, most of the parts can be combined into custom specific switch assemblies. The cost of a ready-to-use assembly as described in this presentation is about 2 x the costs of a comparable thyratron including driver- and heating circuit. (Status Y 2000) The main advantage of the solid state version is the more than 10 x longer life-time, practically no need for maintenance, no restrictions in positioning, and is environmental clean as there is no mercury inside.

10) CONCLUSION

It has been shown that ABB Semiconductors AG produces a range of specific designed components assembled as complete switches which are fulfilling a wide demand for repetitive use in Pulse Power. Circuit requirements and reliability considerations make it favorable to realize a very close interaction between the power semiconductor device, driver-unit, power supply and mounting stack. The switches, which ABB has designed, can replace thyratrons and ingnitrons for medium pulse repetition rates, and offer higher reliability in combination with almost no maintenance.

ABB ABB Semiconductors AG, Fabrikstrasse 3, CH-5600 Lenzburg, Switzerland
Tel.: +41-79-540-9381 / Fax: +41-62-888-6310 / E-mail: pulsepower.abbsem@ch.abb.com
Date: 04.2001 / Adriaan Welleman